International Journal of Nanomedicine

Dovepress
open access to scientific and medical research

Open Access Full Text Article

ORIGINAL RESEARCH

Self-assembling surfactant-like peptide A_6K as potential delivery system for hydrophobic drugs

International Journal of Nanomedicine downloaded from https://www.dovepress.com/
For personal use only.

This article was published in the following Dove Press journal:
International Journal of Nanomedicine
23 January 2015
Number of times this article has been viewed

Yongzhu Chen[1]
Chengkang Tang[2]
Jie Zhang[2]
Meng Gong[3]
Bo Su[2]
Feng Qiu[4]

[1]Periodical Press, [2]Core Facility of West China Hospital, [3]Laboratory of Endocrinology and Metabolism, West China Hospital, [4]Laboratory of Anaesthesia and Critical Care Medicine, Translational Neuroscience Centre, West China Hospital, Sichuan University, Chengdu, People's Republic of China

Background: Finding a suitable delivery system to improve the water solubility of hydrophobic drugs is a critical challenge in the development of effective formulations. In this study, we used A_6K, a self-assembling surfactant-like peptide, as a carrier to encapsulate and deliver hydrophobic pyrene.

Methods: Pyrene was mixed with A_6K by magnetic stirring to form a suspension. Confocal laser scanning microscopy, transmission electron microscopy, dynamic light scattering, atomic force microscopy, fluorescence, and cell uptake measurements were carried out to study the features and stability of the nanostructures, the state and content of pyrene, as well as the pyrene release profile.

Results: The suspension formed contained pyrene monomers trapped in the hydrophobic cores of the micellar nanofibers formed by A_6K, as well as nanosized pyrene crystals wrapped up and stabilized by the nanofibers. The two different encapsulation methods greatly increased the concentration of pyrene in the suspension, and formation of pyrene crystals wrapped up by A_6K nanofibers might be the major contributor to this effect. Furthermore, the suspension system could readily release and transfer pyrene into living cells.

Conclusion: A_6K could be further exploited as a promising delivery system for hydrophobic drugs.

Keywords: pyrene, self-assembling peptide, micelles, nanofibers, drug delivery

Introduction

In the list of popular pharmaceutical chemicals, there are many important hydrophobic drugs, such as doxorubicin and paclitaxel for cancer chemotherapy and propofol for general anesthesia. Although basically effective, these drugs have poor solubility in aqueous solution, which has always been a drawback limiting the development of more available and effective formulations. For this reason, much research has been conducted to increase the solubility and thus the bioavailability of these hydrophobic drugs. Despite the success of novel strategies such as soluble derivatives or prodrugs,[1–3] the strategy using a delivery system is still a predominant approach, particularly considering its potential to achieve targeted delivery or codelivery of different components.[4–6] In recent years, various types of materials have been investigated as delivery systems for hydrophobic drugs, including, but not limited to, liposomes,[7] polymeric nanoparticles,[8–10] hydrogels,[11,12] and carbon nanotubes.[13–15] Several well-studied materials have been developed into clinically available formulations, such as Abraxane® and Doxil®.[16,17] At the same time, a category of self-assembling peptides as novel nanomaterials has emerged in the past decade with advanced properties in

Correspondence: Feng Qiu
Laboratory of Anaesthesia and Critical Care Medicine, Translational Neuroscience Centre, West China Hospital, Sichuan University, Chengdu 610041, People's Republic of China
Tel +86 28 8516 4075
Fax +86 28 8516 4075
Email fengqiu@scu.edu.cn

© 2015 Chen et al. This work is published by Dove Medical Press Limited, and licensed under Creative Commons Attribution – Non Commercial (unported, v3.0) License. The full terms of the License are available at http://creativecommons.org/licenses/by-nc/3.0/. Non-commercial uses of the work are permitted without any further permission from Dove Medical Press Limited, provided the work is properly attributed. Permissions beyond the scope of the License are administered by Dove Medical Press Limited. Information on how to request permission may be found at: http://www.dovepress.com/permissions.php

many fields.[18,19] Based on their chemical structures, self-assembling peptides could form different nanostructures including nanoparticles, nanotubes, and nanofibers, which are also potential carriers for drug delivery.[20–26] It has been demonstrated that nanostructures with a high aspect ratio are advantageous as drug carriers;[27,28] however, on the other hand, their drug loading capacity (LC) is usually very low,[24,29] which has hampered the development of a drug delivery system based on these nanomaterials.

Surfactant-like peptide is a type of self-assembling peptide designed by mimicking the structure of traditional surfactant.[30–32] A_6K, one of the simplest surfactant-like peptides, is composed of six hydrophobic alanines and one hydrophilic lysine. When first introduced about 10 years ago, A_6K and other surfactant-like peptides were observed to form bilayered nanovesicles and nanotubes, which were expected to be potential carriers for biological molecules.[33] On the other hand, a series of investigations has demonstrated that A_6K and other surfactant-like peptides could bind with the hydrophobic section of membrane proteins and stabilize their structure in aqueous solution,[34–36] which essentially confirmed that they could be potential carriers for hydrophobic substances. Recently, our group found that, when directly dissolved in pure water, A_6K could form micellar nanofibers with a hydrophobic core and a very high aspect ratio,[37] indicating that it should be investigated as a possible delivery system for hydrophobic drugs.

Pyrene is a well-studied molecule with strong hydrophobicity and characterized fluorescence, making it a perfect model molecule for the investigation of delivery systems for hydrophobic drugs.[38–42] In this study, we used A_6K to encapsulate pyrene in water suspension. The nanostructures of pyrene-A_6K complex were studied, and then the content and fluorescence properties of encapsulated pyrene were analyzed. Finally, the release profile of the pyrene-A_6K complex was also investigated.

Materials and methods

Encapsulation of pyrene by A_6K

A_6K (peptide sequence Ac-AAAAAAK-$CONH_2$) with a purity of over 95% was commercially synthesized (Shanghai Bootech BioScience and Technology Co Ltd, Shanghai, People's Republic of China). Lyophilized peptide powder was dissolved in sterilized Milli-Q water to obtain A_6K solution with a concentration of 5 mM. Exceeded amount of pyrene (about 5 mg) was put into 5 mL of A_6K solution or Milli-Q water and stirred magnetically for 6 hours. The obtained mixture of A_6K and pyrene was kept in the dark for 4 days to precipitate large particles and obtain a stable upper suspension that was used for further investigations. In order to remove large pyrene nanoparticles from the suspension and to investigate the encapsulating mechanism further, part of the suspension was centrifuged at 2,500× *g* for 15 minutes, and the supernatant was collected and studied in succeeding experiments and compared with the suspension. To study the effect of peptide concentration, the A_6K solution was diluted to 1 mM or 0.2 mM with Milli-Q water, and the suspension/supernatant was obtained as described above. All treatments were carried out at room temperature.

Confocal laser scanning microscopy

Based on the fluorescence of pyrene, confocal laser scanning microscopy (CLSM) (A1Si, Nikon, Tokyo, Japan) was used to observe possible pyrene-containing structures in the suspension and the supernatant. Ten microliters of each sample was dropped onto a clean glass slide and a cover glass slip was put on it to form a thin layer of liquid. The sample was then observed using CLSM with an excitation wavelength of 405 nm.

Transmission electron microscopy

To observe the detailed nanostructures in the suspension and the supernatant by transmission electron microscopy (TEM), a copper grid covered with carbon film was put on the surface of a small drop of suspension or supernatant to absorb a certain amount of sample on it, which was then negatively stained with phosphotungstic acid for about 2 minutes. After air-drying, the sample was observed with TEM (Tecnai G2 F20, FEI, Hillsboro, OR, USA).

Dynamic light scattering

Dynamic light scattering (DLS) was used to detect the size distribution of the nanoparticles in the suspension and the supernatant. One milliliter of each sample was put into a ZEN0112-low volume disposable sizing cuvette and kept at equilibrium at 25°C for 2 minutes prior to measurement. Intensity data were collected as a size-versus-fraction distribution plot using a Zetasizer Nano-ZS instrument (Malvern Instruments, Malvern, UK), with water (refractive index 1.33) chosen as the dispersant. For each measurement, the result was the average of 16–20 collections, and each sample was measured three times to obtain similar results. In order to keep their original states, both samples were measured without further treatment.

Measurement of fluorescence

To study the state of pyrene in the suspension and supernatant, 1 mL of each sample was put into a quartz cuvette and the fluorescence was measured using a spectrophotometer (F-7000, Hitachi, Tokyo, Japan) with the following parameters: excitation wavelength 336 nm, emission wavelength 360–600 nm, excitation slit width 20 nm, emission slit width 2.5 nm, scan speed 240 nm/min, and response time 0.5 seconds.

Determination of pyrene concentration

The concentration of pyrene in the suspension and supernatant was determined by monitoring the I1 fluorescence peak at 374 nm. A calibration curve was constructed by measuring the I1 fluorescence values of a series of standard pyrene solutions dissolved in ethanol (Supplementary data, Figure S1). Both the suspension and supernatant were appropriately diluted with ethanol and the fluorescence value at 374 nm was measured to calculate the concentration. At each peptide concentration, three separate batches of samples were prepared and measured, and statistical results were obtained as the mean ± standard deviation.

Atomic force microscopy

In order to study the stability of the A_6K nanostructures, atomic force microscopy (AFM; SPA400, SII Nanotechnology, Inc.) was used to compare the nanostructures before and after exposure to serum proteins. Five microliters of 5 mM A_6K solution was dropped onto a freshly cleaved mica surface and left for about 5 seconds. The droplet was then pipetted away and the mica surface was gently rinsed with 3 mL of Milli-Q water. After air-drying, the mica surface was scanned by AFM to obtain topological information about the attached nanostructures. The mica sheet was then immersed in Dulbecco's Modified Eagle's Medium supplemented with 10% fetal bovine serum. After incubation at 37°C for 3 days, the mica sheet was removed, and its surface was gently rinsed with 3 mL of Milli-Q water and scanned by AFM.

Release of pyrene

Pyrene release from the suspension was investigated in a phosphate-buffered saline system. One milliliter of suspension was sealed into a dialysis tube (molecular weight cutoff 500–1,000 Da, Beijing Solarbio Science & Technology Co Ltd, Beijing, People's Republic of China) and dialyzed against 100 mL of 0.02 M phosphate-buffered saline (pH 7.4). At appropriate intervals ($t_{1, 2, 3 \ldots 11}$=0.2, 0.5, 1, 2, 4, 6, 8, 12, 25, 50, 75 hours), 1 mL of solution was removed from the release medium, and replaced immediately with 1 mL of fresh phosphate-buffered saline. For each interval, the concentration of pyrene released was determined by a fluorescence method similar to that described above, except that an alternative calibration curve was constructed using a standard pyrene solution in phosphate-buffered saline (Supplementary data, Figure S2), and all samples were measured without further dilution. When maximum release was reached, the cumulative release at each time point was calculated as follows:

$$\text{Cumulative release} = \frac{C_n \times 100 + \sum_{i=1}^{n-1} C_i}{C_{11} \times 100 + \sum_{i=1}^{10} C_i} \times 100\% \quad (1)$$

where C_n is the pyrene concentration at t_n, C_i is the pyrene concentration at t_i, and C_{11} is the maximum pyrene concentration reached at the end of the experiment.

Delivery of pyrene

Human hepatocellular carcinoma (HepG2) cells were used to test if the suspension could release and delivery pyrene to cultured cells. HepG2 cells were conventionally cultured to confluence, harvested, and adjusted to a density of 1×10^6 per mL. One milliliter of cells were transferred into a well of a 12-well plate, into which 20 μL of the suspension was added. The system was then gently shaken in a carbon dioxide cell incubator for 4 hours, after which the cells were rinsed in phosphate-buffered saline three times and resuspended in the same volume of phosphate-buffered saline. Next, 10 μL of cells was removed and dropped onto a clean glass slide, covered with a cover glass slip, and observed by CLSM with an excitation wavelength of 405 nm.

Results and discussion

Formation of pyrene suspension

Pyrene is a hydrophobic drug with extremely low solubility in H_2O, so after stirring in Milli-Q water for 6 hours, the crystals of pyrene were poorly dissolved, sticking to the wall of the bottle, floating on the water surface, or precipitating at the bottom of the bottle. When the pyrene is stirred in A_6K solution, it dispersed rapidly and formed a thick milky mixture. LSCM and TEM showed that this mixture contained many large pyrene particles (Supplementary data, Figures S3 and S4). While standing in the dark for 4 days, the mixture underwent slow precipitation and became clearer, and finally formed a stable milky suspension (Figure 1). The suspension

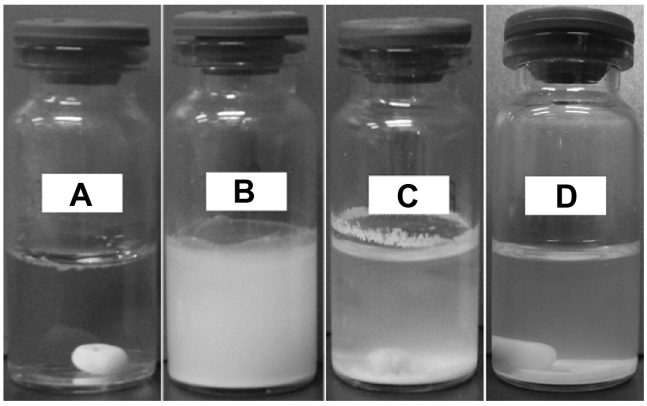

Figure 1 Formation of suspension by pyrene-A_6K.
Notes: (**A**) Pyrene crystals could not be dispersed in pure water. (**B**) Pyrene stirred with A_6K forms a milky mixture and undergoes precipitation during storage. (**C**) Intermediate state of suspension after 2 days. (**D**) Suspension formed after 4 days.

was deemed to be stable when its appearance did not change dramatically and its fluorescence spectrum reached an equilibrium state (Supplementary data, Figure S5).

Fluorescent particles observed by CLSM

By using CLSM, it was found that the suspension contained numerous fluorescent pyrene particles (Figure 2). Although the particles varied in terms of shape and size, they all seemed to be smaller than micron size, ie, much smaller than insoluble pyrene crystals. In contrast, the supernatant showed no obvious fluorescence (data not shown), indicating that fluorescent particles were removed after centrifugation. It should be noted that because of the diffusion of fluorescence and the limited magnification afforded by optical microscopy, details of the structure and size of pyrene particles could not be determined accurately by CLSM.

Character of nanostructures

We then used TEM to further study the nanostructures in the suspension and supernatant. As shown in Figure 3A–C, the suspension contained nanoparticles no more than 100 nm in size that were wrapped up in dense nanofibers. These nanofibers were morphologically similar to what was observed for pure A_6K in our previous work,[37] with an estimated diameter of 5–10 nm and length of several microns. However, the morphology of nanoparticles was somewhat diverse, particularly when TEM samples were prepared in different batches. The approximate diameter of the nanoparticles varied from 10 to 100 nm (Figure 3A and C), with an average of 43.61±27.03 nm (n=50). Further, smaller nanoparticles could form aggregates with a size of more than hundreds of nanometers (Figure 3B). Nanostructures in the supernatant were also observed by TEM. As shown in Figure 3D, all large particles in the supernatant had been effectively removed and only long nanofibers were observed.

The size distributions in the suspension and the supernatant were also characterized by DLS. As shown in Figure 4, the size distribution in the suspension was predominantly around 400–1,000 nm, with a polydispersity index of 0.496±0.078 (mean ± SD), while the size distribution in the supernatant appeared to be around 30–70 nm and 200–600 nm, with a polydispersity index of 0.275±0.053. It should be pointed out that the size distribution data obtained by DLS were somewhat different from the results estimated on the TEM images. A possible reason for this difference is that DLS, as a method to measure the size of granular structures, could not accurately reflect the size of nanofibers with a high aspect ratio, which were predominant in both samples and affected the results obtained by DLS. However, the DLS results clearly showed that after centrifugation, the size distribution of the supernatant was obviously narrower than that of the suspension. Further, the size distribution of the supernatant was very similar to that of pure A_6K reported in our previous study which was characterized by the distribution around 30–70 nm.[37] These results further indicated that,

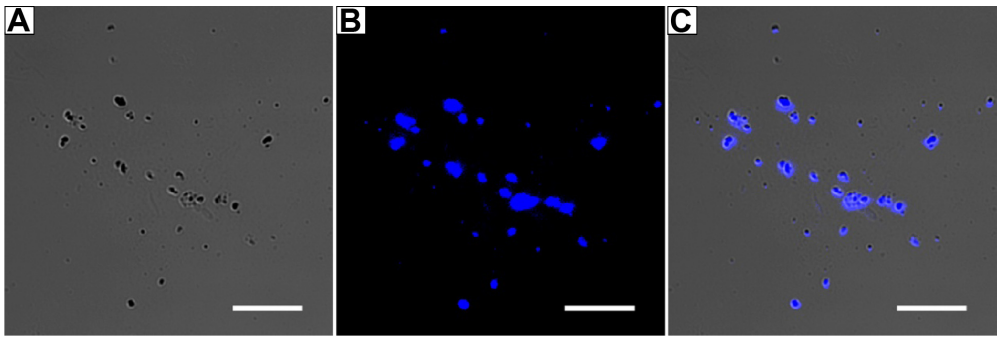

Figure 2 Fluorescent pyrene particles in suspension.
Notes: (**A**) Nanoparticles under normal light. (**B**) Obvious fluorescence could be seen by confocal laser scanning microscopy. (**C**) Merged image showing that all nanoparticles are fluorescent pyrene particles. Scale bar, 5 μm.

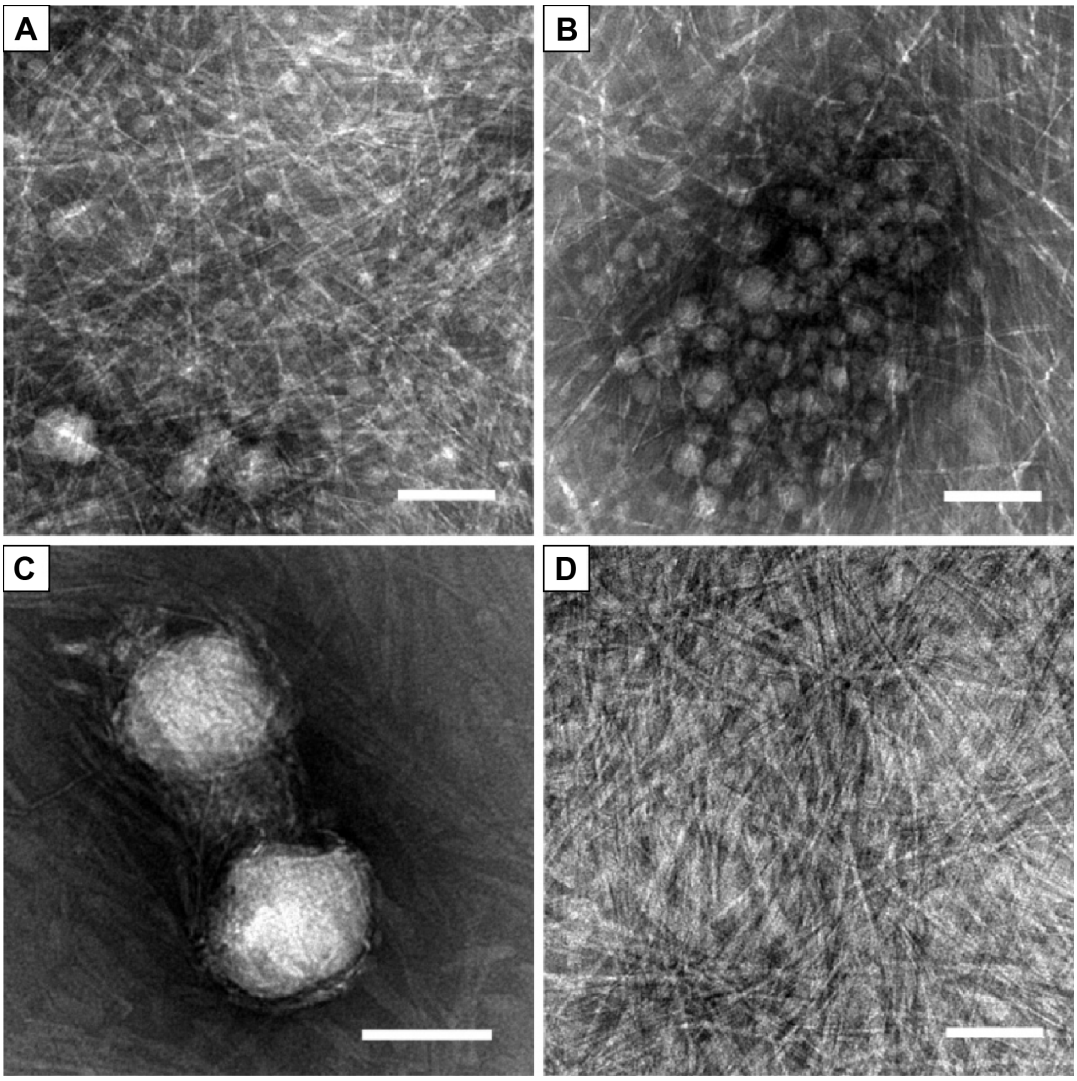

Figure 3 Transmission electron microscopic images of nanostructures in the suspension and supernatant.
Notes: (**A**–**C**) Nanostructures in the suspension. (**A**, **B**) were from the same sample, showing A_6K nanofibers as well as nanoparticles with a diameter of tens of nanometers. (**C**) Larger pyrene particles with a diameter of about 100 nm were observed in another transmission electron microscopy sample. (**D**) Only A_6K nanofibers were present in the supernatant. Scale bar, 100 nm.

after centrifugation, large nanoparticles were effectively removed from the sample and the suspension contained only nanofibers. On the other hand, TEM and DLS measurements showed that the size distribution of the nanoparticles had high polydispersity.

Two states of pyrene indicated by fluorescence spectra

Although the results of the morphological studies reported above confirm the existence of nanosized pyrene particles wrapped up in A_6K nanofibers, it is not clear if there were smaller pyrene molecules encapsulated in the hydrophobic cores of these nanofibers. For this reason, the pyrene fluorescence spectra of the suspension and supernatant were measured, and clearly showed the existence and state of pyrene in both samples. As shown in Figure 5, the fluorescence spectrum for the suspension revealed the existence of pyrene in two different states. Peaks seen at 360–440 nm indicated pyrene monomers, while peaks seen at 440–500 nm indicated the existence of pyrene excimers, ie, the nanosized pyrene particles described above. In the fluorescence spectrum for the supernatant, the absence of an excimer peak indicated the absence of pyrene particles, which is consistent with the results of the morphological studies. However, the spectrum for the supernatant also showed peaks for the pyrene monomer similar to those of the suspension, indicating that the supernatant also contained pyrene in the form of a monomer. Further, the I1/I3 values

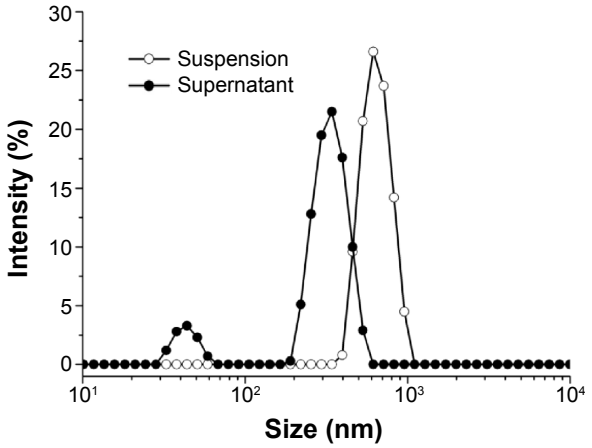

Figure 4 Size distribution of nanostructures in the suspension and supernatant. The change in size distribution indicates the absence of pyrene nanoparticles in the supernatant.

for the suspension and supernatant were calculated to be 1.39 and 1.50, respectively, both of which were lower than that for pyrene in a polar water solution (about 1.7), indicating that the pyrene monomers in both samples were trapped in a hydrophobic environment.

Proposed model for encapsulating mechanism

Based on the results described above, a model was proposed to demonstrate the mechanism via which pyrene was encapsulated by A_6K. As shown in Figure 6, with its typical amphiphilic structure, A_6K can self-assemble to form cylindrical micelles with a hydrophobic core, which could serve as a reservoir for hydrophobic pyrene monomers. However, because the compact packing of the hydrophobic region

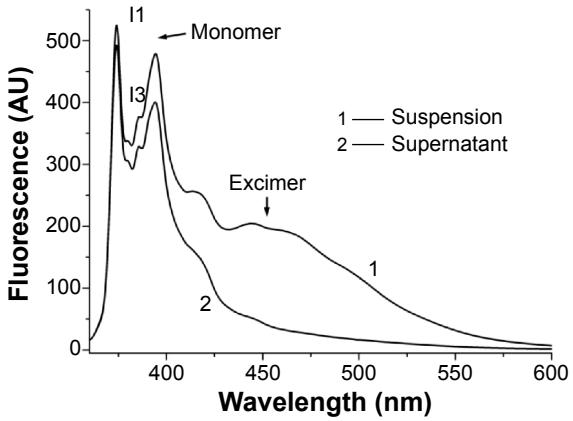

Figure 5 Fluorescence spectra for the suspension and supernatant. Coexistence of a monomer peak and an excimer peak indicates that pyrene exists in suspension in the two states. The absence of an excimer peak in the supernatant indicates the absence of pyrene nanoparticles.
Abbreviation: AU, absorbance units.

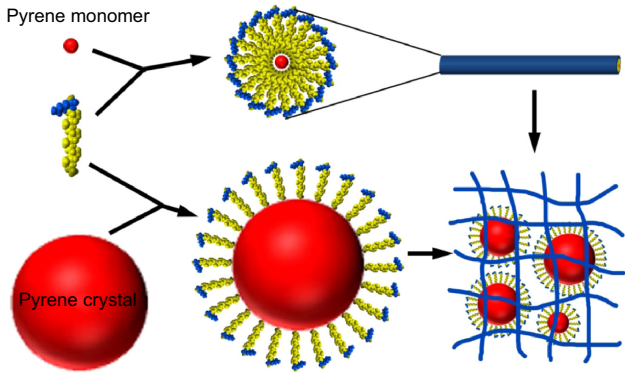

Figure 6 Proposed model for encapsulation of pyrene. The pyrene monomer could be trapped in the hydrophobic core of the A_6K micellar nanofibers, and pyrene crystals could be wrapped up by many of these nanofibers.

leaves limited space inside the micelles, the encapsulating efficiency of this mode is assumed to be very low. In contrast, larger pyrene crystals could be surrounded by free peptide monomers with their hydrophobic tails attaching to the surface of pyrene. This is similar to what has been described for surfactant-like peptides encapsulating membrane proteins.[36] The pyrene-peptide complex could be further wrapped up by nanofibers, which might be helpful for dispersing and stabilizing pyrene crystals in the suspension. In this model, pyrene could be encapsulated by A_6K in two different states, allowing more pyrene to be encapsulated.

Increased pyrene concentration and loading capacity

As determined by the fluorescence method, the concentration of pyrene in the supernatant was 0.047±0.0053 mM, which was two orders of magnitude higher than the concentration of pyrene in saturated water solution (about 7×10^{-4} mM, as reported elsewhere[43]), while in the suspension, the concentration of pyrene was 0.655±0.045 mM, which was a further order of magnitude higher. The LC was then calculated as follows:

$$\mathrm{LC} = \frac{C_p \times W_p}{C_p \times W_p + C_a \times W_a} \times 100\% \qquad (2)$$

where C_p is the concentration of pyrene, W_p is the molecule weight of pyrene (202.26 Da), C_a is the concentration of A_6K (5 mM in our study), and W_a is the molecular weight of A_6K (613.73 Da). According to the equation, when only pyrene in the supernatant was counted, the LC was 0.31%. When pyrene in the suspension was counted, the LC was markedly increased to 4.14%.

Effect of peptide concentration

Before studying the pyrene-peptide system further, we investigated the effect of peptide concentration on the system. Because the A_6K concentration of 5 mM used in the above study was already close to saturation, the original peptide solution was diluted to 1 mM or 0.2 mM and used instead of 5 mM A_6K to encapsulate pyrene. When the peptide concentration was 1 mM, TEM showed a nanofiber network with decreased density that could still encapsulate pyrene nanoparticles with an average size of 32.27±18.56 nm (n=50). However, both the photographic and TEM results for the suspension showed that a smaller amount of pyrene nanoparticles was encapsulated in 1 mM A_6K (Figure 7A and B). When the peptide concentration was diluted to 0.2 mM, which was just a little higher than its critical micelle concentration (0.1 mM, as reported elsewhere[37]), no obvious suspension was formed and TEM revealed very few nanofibers without nanoparticles entrapped within (Figure 7C). Further, Figure 7D indicates a decrease in the concentration of pyrene with decreasing peptide concentration. These results suggest that the density of the nanofibers as determined by peptide concentration was the predominant parameter affecting encapsulation efficacy, supporting the model proposed above.

Stability of A_6K nanofibers

In a previous study, we showed that A_6K nanofibers were sensitive to extreme pH and high temperature conditions. However, considering their potential biological application,

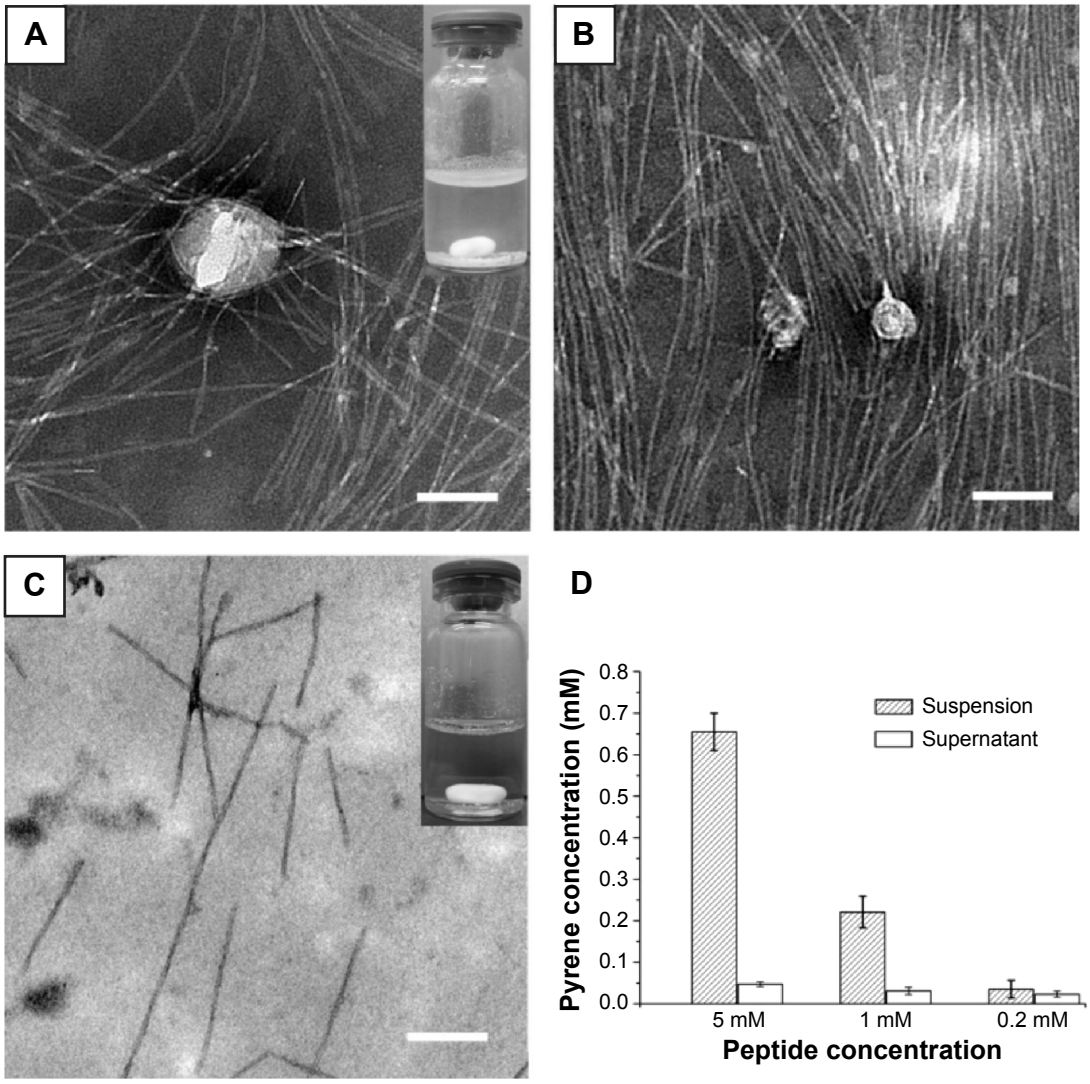

Figure 7 Encapsulation of pyrene by 1 mM or 0.2 mM A_6K.
Notes: (**A**, **B**) show that the densities of the A_6K nanofibers and encapsulated pyrene particles were decreased compared with those in 5 mM A_6K. (**C**) Very few nanofibers were observed in 0.2 mM A_6K, with no pyrene particles encapsulated. The inserts in (**A**) and (**C**) show photographic images of the corresponding suspension. (**D**) The pyrene concentration decreased markedly as the concentration of A_6K decreased. Scale bar, 100 nm.

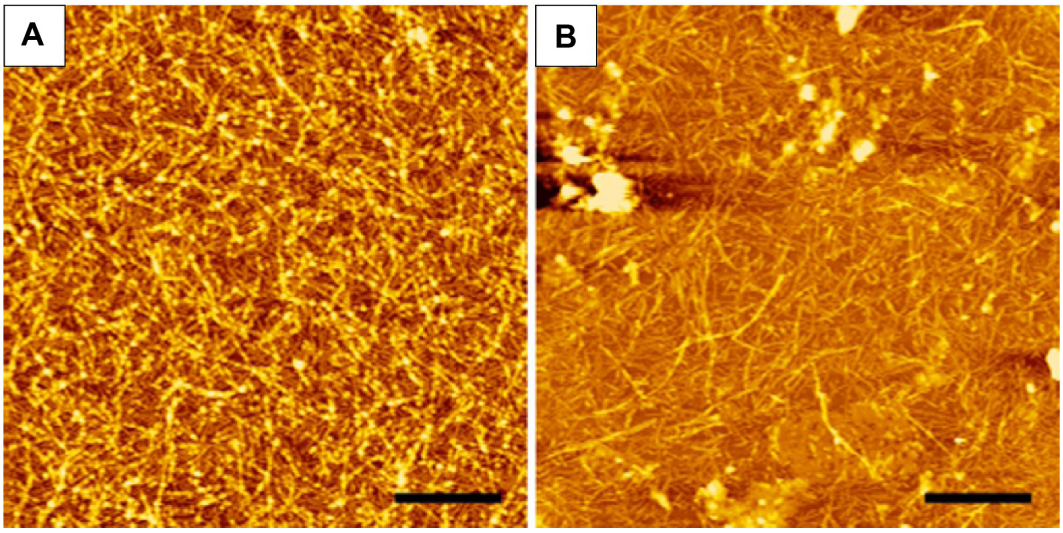

Figure 8 Stability of A_6K nanofibers.
Notes: (**A**) Atomic force microscopic image of freshly prepared A_6K nanofibers. (**B**) A_6K nanofibers after incubation in Dulbecco's Modified Eagle's Medium supplemented with 10% fetal bovine serum. Scale bar, 1 μm.

we needed to determine their stability in mild physiological conditions. As shown in Figure 8, after incubation in cell culture medium, nanofibers attached onto a mica surface remained assembled, indicating that physiological pH and presence of serum protein could not change or destroy the self-assembling nanostructure of A_6K, establishing it as an ideal material for drug delivery.

Release and transfer of pyrene

We then studied the release profile of the suspension obtained with 5 mM A_6K. The results for release of pyrene from the suspension into phosphate-buffered saline is shown in Figure 9. In the first 12 hours, the system showed a very fast release profile, with about 90% of pyrene released. After 12 hours, release of pyrene became very slow and an equilibrium state was reached after 75 hours. This two-stage release profile is consistent with the two-state encapsulating mode: most of the pyrene crystals wrapped up by the nanofibers would be released easily and more rapidly, and the small amount of pyrene monomers encapsulated in the core of the nanofibers would be released very slowly.

Finally we used HepG2 cells as a model to study if our system could release and transfer pyrene into living cells. As shown in Figure 10, after incubation with the pyrene-A_6K suspension, HepG2 cells showed obvious pyrene fluorescence, indicating that pyrene could be readily released from the complex in the suspension and effectively transferred into the cells.

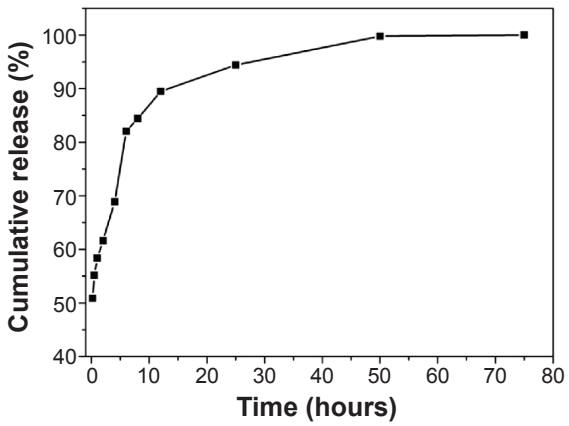

Figure 9 Release profile for pyrene from the suspension. Rapid release occurred in the first 12 hours, after which pyrene was slowly released until an equilibrium state was reached.

Conclusion

Using surfactant-like peptide A_6K as a carrier material and pyrene as a model drug, we have identified a potential encapsulation and delivery system for hydrophobic agents. It was found that pyrene could be encapsulated by A_6K in two different modes, ie, either trapped in the hydrophobic cores of micellar nanofibers as monomers or wrapped up by nanofibers as nanosized crystals. This two-state encapsulating model, in particular wrapping up by nanofibers, could greatly increase the concentration of pyrene as well as the LC of the system. Further, the encapsulated pyrene could be readily released and transferred into living cells. These results suggest that surfactant-like peptides such as A_6K could be a promising type of nanomaterial for the encapsulation and

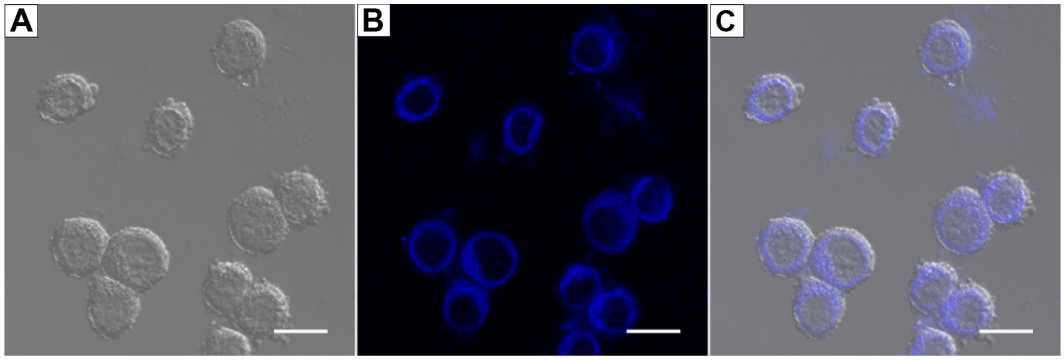

Figure 10 Transfer of pyrene into HepG2 cells.
Notes: (**A**) Cells observed under normal light. (**B**) Obvious fluorescence was observed by confocal laser scanning microscopy. (**C**) Merged image showing that fluorescent pyrene particles were transferred into cells. Scale bar, 20 μm.

delivery of hydrophobic drugs. Considering the fact that these peptides could be easily modified to have additional functions such as targeted delivery, it is very attractive to exploit drug delivery system based on surfactant-like peptides. However, our current work is mainly focused on the basic encapsulating mechanism, and more detailed parameters, such as the amount of pyrene and duration and speed of stirring, have not been investigated. In order to develop a drug delivery system based on our findings, more work needs to be carried out to optimize and standardize this procedure.

Acknowledgment

This work was financially supported by the National Natural Science Foundation of China (81000658 and 31100565).

Disclosure

The authors report no conflicts of interest in this work.

References

1. Li NN, Lin J, Gao D, Zhang LM. A macromolecular prodrug strategy for combinatorial drug delivery. *J Colloid Interface Sci.* 2014;417:301–309.
2. Zhou Y, Yang J, Liu J, Wang Y, Zhang WS. Efficacy comparison of the novel water-soluble propofol prodrug HX0969w and fospropofol in mice and rats. *Br J Anaesth.* 2013;111:825–832.
3. Gu Y, Zhong Y, Meng F, Cheng R, Deng C, Zhong Z. Acetal-linked paclitaxel prodrug micellar nanoparticles as a versatile and potent platform for cancer therapy. *Biomacromolecules.* 2013;14:2772–2780.
4. Yu P, Xia XM, Wu M, et al. Folic acid-conjugated iron oxide porous nanorods loaded with doxorubicin for targeted drug delivery. *Colloids Surf B Biointerfaces.* 2014;120:142–151.
5. Li Q, Lv S, Tang Z, et al. A co-delivery system based on paclitaxel grafted mPEG-b-PLG loaded with doxorubicin: preparation, in vitro and in vivo evaluation. *Int J Pharm.* 2014;471:412–420.
6. Hira SK, Mishra AK, Ray B, Manna PP. Targeted delivery of doxorubicin-loaded poly (epsilon-caprolactone)-b-poly (N-vinylpyrrolidone) micelles enhances antitumor effect in lymphoma. *PLoS One.* 2014;9:e94309.
7. Chen J, Lu WL, Gu W, et al. Drug-in-cyclodextrin-in-liposomes: a promising delivery system for hydrophobic drugs. *Expert Opin Drug Deliv.* 2014;11:565–577.
8. Li F, Zhu A, Song X, Ji L. Novel surfactant for preparation of poly(L-lactic acid) nanoparticles with controllable release profile and cyto-compatibility for drug delivery. *Colloids Surf B Biointerfaces.* 2014;115:377–383.
9. Byagari K, Shanavas A, Rengan AK, Kundu GC, Srivastava R. Biocompatible amphiphilic pentablock copolymeric nanoparticles for anti-cancer drug delivery. *J Biomed Nanotechnol.* 2014;10:109–119.
10. Battogtokh G, Ko YT. Self-assembled polymeric nanoparticle of PEGylated chitosan-ceramide conjugate for systemic delivery of paclitaxel. *J Drug Target.* 2014;22:813–821.
11. Perez E, Fernandez A, Olmo R, Teijon JM, Blanco MD. pH and glutathion-responsive hydrogel for localized delivery of paclitaxel. *Colloids Surf B Biointerfaces.* 2014;116:247–256.
12. Cho JK, Kuh HJ, Song SC. Injectable poly(organophosphazene) hydrogel system for effective paclitaxel and doxorubicin combination therapy. *J Drug Target.* 2014;22:761–777.
13. Tsai HC, Lin JY, Maryani F, Huang CC, Imae T. Drug-loading capacity and nuclear targeting of multiwalled carbon nanotubes grafted with anionic amphiphilic copolymers. *Int J Nanomedicine.* 2013;8:4427–4440.
14. Arya N, Arora A, Vasu KS, Sood AK, Katti DS. Combination of single walled carbon nanotubes/graphene oxide with paclitaxel: a reactive oxygen species mediated synergism for treatment of lung cancer. *Nanoscale.* 2013;5:2818–2829.
15. Gu YJ, Cheng J, Jin J, Cheng SH, Wong WT. Development and evaluation of pH-responsive single-walled carbon nanotube-doxorubicin complexes in cancer cells. *Int J Nanomedicine.* 2011;6:2889–2898.
16. Bertrand N, Wu J, Xu X, Kamaly N, Farokhzad OC. Cancer nanotechnology: the impact of passive and active targeting in the era of modern cancer biology. *Adv Drug Deliv Rev.* 2014;66:2–25.
17. Dawidczyk CM, Kim C, Park JH, et al. State-of-the-art in design rules for drug delivery platforms: lessons learned from FDA-approved nanomedicines. *J Control Release.* 2014;187:133–144.
18. Lakshmanan A, Zhang S, Hauser CA. Short self-assembling peptides as building blocks for modern nanodevices. *Trends Biotechnol.* 2012;30:155–165.
19. Liu J, Zhao X. Design of self-assembling peptides and their biomedical applications. *Nanomedicine (Lond).* 2011;6:1621–1643.
20. Lv S, Tang Z, Li M, et al. Co-delivery of doxorubicin and paclitaxel by PEG-polypeptide nanovehicle for the treatment of non-small cell lung cancer. *Biomaterials.* 2014;35:6118–6129.
21. Liu J, Xu H, Zhang Y, et al. Novel tumor-targeting, self-assembling peptide nanofiber as a carrier for effective curcumin delivery. *Int J Nanomedicine.* 2014;9:197–207.

22. Zhang P, Cheetham AG, Lin YA, Cui H. Self-assembled Tat nanofibers as effective drug carrier and transporter. *ACS Nano.* 2013;7:5965–5977.
23. Sadatmousavi P, Mamo T, Chen P. Diethylene glycol functionalized self-assembling peptide nanofibers and their hydrophobic drug delivery potential. *Acta Biomater.* 2012;8:3241–3250.
24. Soukasene S, Toft DJ, Moyer TJ, et al. Antitumor activity of peptide amphiphile nanofiber-encapsulated camptothecin. *ACS Nano.* 2011;5:9113–9121.
25. Liu J, Zhang L, Yang Z, Zhao X. Controlled release of paclitaxel from a self-assembling peptide hydrogel formed in situ and antitumor study in vitro. *Int J Nanomedicine.* 2011;6:2143–2153.
26. Keyes-Baig C, Duhamel J, Fung SY, Bezaire J, Chen P. Self-assembling peptide as a potential carrier of hydrophobic compounds. *J Am Chem Soc.* 2004;126:7522–7532.
27. Li SD, Huang L. Pharmacokinetics and biodistribution of nanoparticles. *Mol Pharm.* 2008;5:496–504.
28. Geng Y, Dalhaimer P, Cai S, et al. Shape effects of filaments versus spherical particles in flow and drug delivery. *Nat Nanotechnol.* 2007; 2:249–255.
29. Lim YB, Lee E, Lee M. Controlled bioactive nanostructures from self-assembly of peptide building blocks. *Angew Chem Int Ed.* 2007;46:9011–9014.
30. Zhang S. Lipid-like self-assembling peptides. *Acc Chem Res.* 2012;45: 2142–2150.
31. Zhao X. Design of self-assembling surfactant-like peptides and their applications. *Curr Opin Colloid Interface Sci.* 2009;14:340–348.
32. Vauthey S, Santoso S, Gong H, Watson N, Zhang S. Molecular self-assembly of surfactant-like peptides to form nanotubes and nanovesicles. *Proc Natl Acad Sci U S A.* 2002;99:5355–5360.
33. Maltzahn G, Vauthey S, Santoso S, Zhang S. Positively charged surfactant-like peptides self-assemble into nanostructures. *Langmuir*. 2003;19:4332–4337.
34. Ge B, Yang F, Yu D, Liu S, Xu H. Designer amphiphilic short peptides enhance thermal stability of isolated photosystem-I. *PLoS One.* 2010;5:e10233.
35. Matsumoto K, Vaughn M, Bruce BD, Koutsopoulos S, Zhang S. Designer peptide surfactants stabilize functional photosystem-I membrane complex in aqueous solution for extended time. *J Phys Chem B.* 2009;113:75–83.
36. Zhao X, Nagai Y, Reeves PJ, Kiley P, Khorana HG, Zhang S. Designer short peptide surfactants stabilize G protein-coupled receptor bovine rhodopsin. *Proc Natl Acad Sci U S A.* 2006;103:17707–17712.
37. Qiu F, Chen Y, Zhao X. Comparative studies on the self-assembling behaviors of cationic and catanionic surfactant-like peptides. *J Colloid Interface Sci.* 2009;336:477–484.
38. Zhang H, Li Z, Xu P, Wu R, Jiao Z. A facile two step synthesis of novel chrysanthemum-like mesoporous silica nanoparticles for controlled pyrene release. *Chem Commun (Camb).* 2010;46:6783–6785.
39. Schatz C, Smith EG, Armes SP, Wanless EJ. Reversible pH-triggered encapsulation and release of pyrene by adsorbed block copolymer micelles. *Langmuir.* 2008;24:8325–8331.
40. Manna U, Patil S. Encapsulation of uncharged water-insoluble organic substance in polymeric membrane capsules via layer-by-layer approach. *J Phys Chem B.* 2008;112:13258–13262.
41. Li F, Wang J, Tang F, et al. Fluorescence studies on a designed self-assembling peptide of RAD16-II as a potential carrier for hydrophobic drug. *J Nanosci Nanotechnol*. 2009;9:1611–1614.
42. Tang F, Zhao X. Interaction between a self-assembling peptide and hydrophobic compounds. *J Biomater Sci Polym Ed.* 2010;21:677–690.
43. Yekta A, Xu B, Duhamel J, Adiwidjaja H, Winnik MA. Fluorescence studies of associating polymers in water: determination of the chain end aggregation number and a model for the association process. *Macromolecules.* 1995;28:956–966.

Supplementary data

Calibration curve for pyrene at higher concentrations in ethanol

Standard pyrene solutions in ethanol were prepared at concentrations ranging from 1×10^{-4} mM to 2×10^{-2} mM. The fluorescence spectrum of each standard solution was measured to obtain its value at 374 nm. The parameters for measurement of fluorescence were set as follows: exciting wavelength 336 nm, scan speed 240 nm/min, excitation slit width 5 nm, emission slit width 5 nm, and photomultiplier tube voltage 400 V. The calibration curve was obtained as a concentration-versus-fluorescence plot (Figure S1), from which the following equation could be obtained:

$$y = 0.00507*\exp(0.00832x) - 0.00504 \quad (1)$$

where y is the pyrene concentration and x is the fluorescence value at 374 nm. The adjusted R-square value is 0.99874.

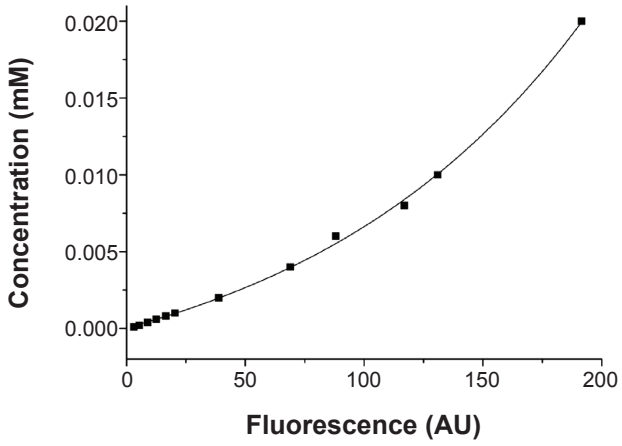

Figure S1 Calibration curve for pyrene at higher concentrations in ethanol.

Calibration curve for pyrene at lower concentrations in phosphate-buffered saline

Standard pyrene solutions in phosphate-buffered saline (0.02 M) were prepared by diluting a stock pyrene solution (1 mM in ethanol) with phosphate-buffered saline, at concentrations ranging from 1×10^{-5} mM to 6×10^{-4} mM. The fluorescence spectrum of each standard solution was measured to obtain its value at 374 nm. Parameters for fluorescence measurement were set as follows: exciting wavelength 336 nm, scan speed 240 nm/min, excitation slit width 20 nm, emission slit width 10 nm, and photomultiplier tube voltage 400 V. The calibration curve was obtained as a concentration-versus-fluorescence plot (Figure S2), according to which the following equation could be obtained:

$$y = 3.9591\times10^{-6}x - 4.48259\times10^{-5} \quad (2)$$

where y is the pyrene concentration and x is the fluorescence value at 374 nm. The adjusted R-square value is 0.99937.

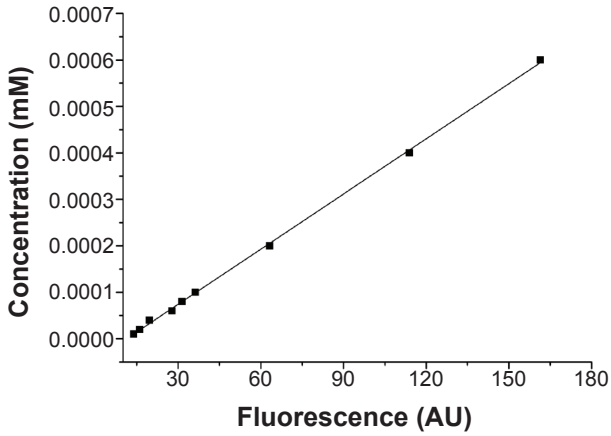

Figure S2 Calibration curve for pyrene at lower concentrations in phosphate-buffered saline.

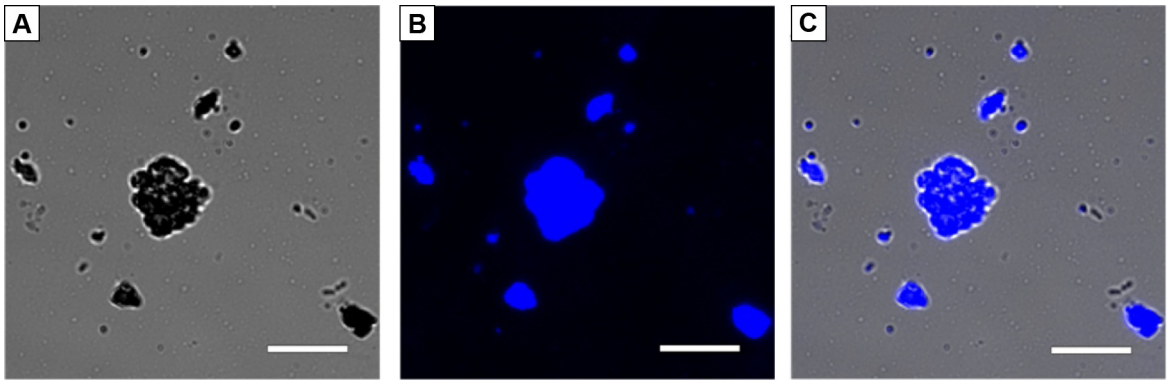

Figure S3 Fluorescent pyrene particles in the initial mixture of pyrene and A_6K.
Notes: (**A**) Normal light, (**B**) fluorescence, and (**C**) merged image. Large pyrene particles could be seen in these images. Scale bar, 5 μm.

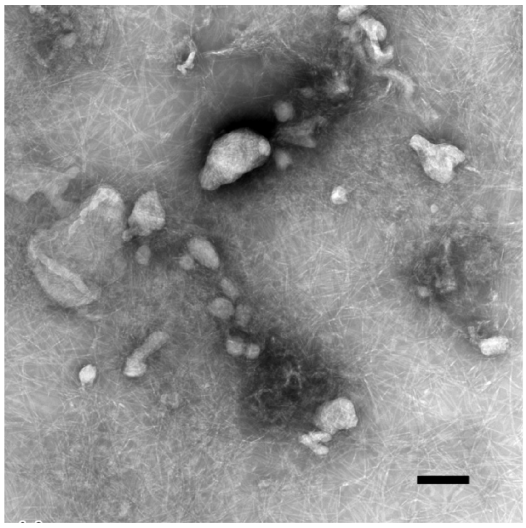

Figure S4 Transmission electron microscopic image of the initial mixture of pyrene and A_6K. Large pyrene particles with an irregular shape can be seen in this image.

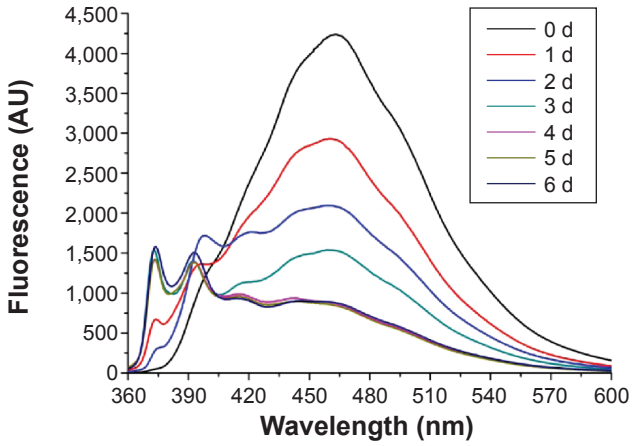

Figure S5 Fluorescence spectra for the pyrene-A_6K mixture at different storage times. In the first 4 days, the fluorescence value between 440–500 nm dropped markedly, indicating the decreasing of pyrene eximers. After 4 days, the spectra reached an equilibrium state, indicating that a stable suspension had been obtained.

International Journal of Nanomedicine

Dovepress

Publish your work in this journal

The International Journal of Nanomedicine is an international, peer-reviewed journal focusing on the application of nanotechnology in diagnostics, therapeutics, and drug delivery systems throughout the biomedical field. This journal is indexed on PubMed Central, MedLine, CAS, SciSearch®, Current Contents®/Clinical Medicine, Journal Citation Reports/Science Edition, EMBase, Scopus and the Elsevier Bibliographic databases. The manuscript management system is completely online and includes a very quick and fair peer-review system, which is all easy to use. Visit http://www.dovepress.com/testimonials.php to read real quotes from published authors.

Submit your manuscript here: http://www.dovepress.com/international-journal-of-nanomedicine-journal